

Effect of Drying Conditions on the Particle Size, Dispersion State, and Mechanical Sensitivities of Nano HMX

Jie Liu,^[a] Wei Jiang,^[a] Fengsheng Li,^{*,[a]} Longxiang Wang,^[a] Jiangbao Zeng,^[a] Qing Li,^[a] Yi Wang,^[a] and Qing Yang^[a]

Abstract: Nano HMX was prepared using a bi-directional rotation mill and dried in different liquids, at various temperatures, and under different conditions. It was revealed that the samples were caked seriously and the particles tend to aggregate with obviously increased size when dried through ordinary drying in different liquids at 70 °C, which also occurred after vacuum drying. The degree of caking and aggregation was enhanced with increasing temperature. The particles were prevented to grow and the samples were fluffy when supercritical drying, particularly

freeze drying, was used. The mechanical sensitivities of the samples marked with I-HMX, O-HMX, and F-HMX, which had average sizes of 120.36 μm , 1.18 μm , and 0.16 μm , respectively, were carried out. Compared with I-HMX, the friction, impact, and shock sensitivities of O-HMX were slightly lower, and a significant sensitivity decrease for F-HMX happened with specific values of 28%, 42.8%, and 56.4%, respectively, which demonstrated significant safety improvement.

Keywords: Drying conditions • Nano HMX • Particle size • Dispersion state • Mechanical sensitivities

1 Introduction

HMX, which has high detonation heat, detonation velocity, and detonation pressure is extensively applied in plastic bonded explosives (PBX) [1–3] and solid rocket propellants [4–9]. However, the high mechanical sensitivities of the industrial HMX (d_{50} = 50–150 μm) restricted its actual applications, and it has become a research focus to reduce their values. The studies showed that the sensitivities of nitramine explosives were affected obviously by the size and its distribution of the explosive particles [10–13]. The impact sensitivities of HMX were effectively reduced by reducing the particle sizes [14], if nanoparticles were obtained, the mechanical sensitivities were significantly decreased [15]. Nano HMX could be prepared by the solvent/nonsolvent recrystallization method [16] and the Rapid Expansion of Supercritical Solution (RESS) method [17]. It was very difficult to realize large-scale production, because of the small capacity of material processing, the complicated technological parameters, and the bad reproducibility of experiments.

Recent research showed that batched preparation for regular nano HMX particles was achieved by a wet ball mill [18]. However, to ensure the safety of mechanical milling, the raw materials must be addressed in liquid environments. The technique to extract the nanoparticles efficiently from the slurry became the key constraint for its application. In this paper, the particle size, dispersion state, and mechanical sensitivities of the dried samples under different conditions were investigated so that an appropriate method for the extraction of nano HMX was found.

2 Experiment

2.1 Preparation of Nano HMX

Industrial HMX, produced by Gansu Yinguang Chemical Industry Group Co, Ltd of China, was dispersed in the aforementioned miscible liquid (mixture of the deionized water, ethanol, and 2-propanol, with a volume ratio of 10:10:1). The suspension containing 500 g HMX with a mass concentration of 15% was put into the bi-directional rotation mill for 5 h, in which the axle and the barrel were rotating reversely and simultaneously. It was designed by Professor F. S. Li [19]. The rotation speeds of the axle and the barrel were held in a range of 90–150 rpm and 60–90 rpm, respectively. The grinding medium was ceramic balls with 0.2–0.4 mm diameter, and its filling content was controlled at a level of 65–70%. During pulverization, the machine was cooled by cycling water. The yield was about 97%.

2.2 Instruments and Devices

A Malvern Zetasizer 3000HSA laser particle size analyzer was used to measure the size distribution of nano HMX

[a] J. Liu, W. Jiang, F. Li, L. Wang, J. Zeng, Q. Li, Y. Wang, Q. Yang
National Special Superfine Powder Engineering Research Center of China
Nanjing University of Science and Technology
No.200, Xiaolingwei, District Xuanwu, Nanjing, 210094 Jiangsu, P. R. China
*e-mail: jie_liu1987@163.com

before drying, the particle size and the morphology were characterized by using a S-4800II Scanning Electron Microscope (SEM). Dried HMX was characterized with a Malvern Mastersizer Micro laser particle size analyzer and a S-4800II Scanning Electron Microscope (SEM), Hitachi High-Technologies Corporation.

A water bath oven, a vacuum oven, supercritical drying equipment, and a vacuum freeze drying device were used to dry the slurry of nano HMX, respectively.

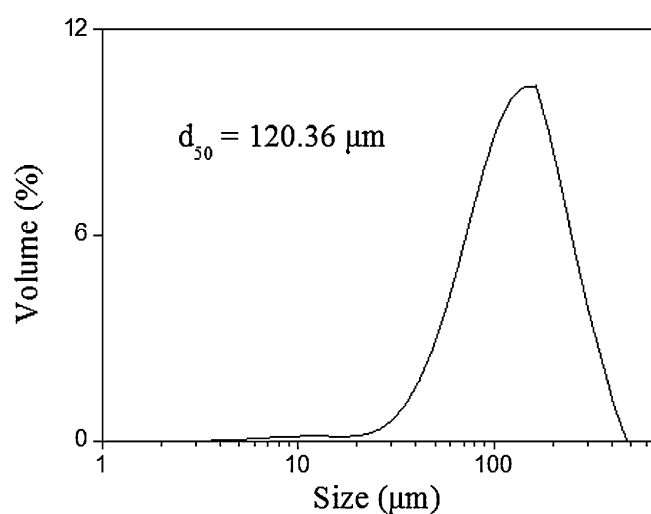
2.3 Supercritical Drying

The suspension was transported to the drying tower at a rate of 6 mL min^{-1} by a pump and atomized by the expanded CO_2 . The liquid was dissolved and carried by CO_2 , discharged in the separation tower, which was maintained

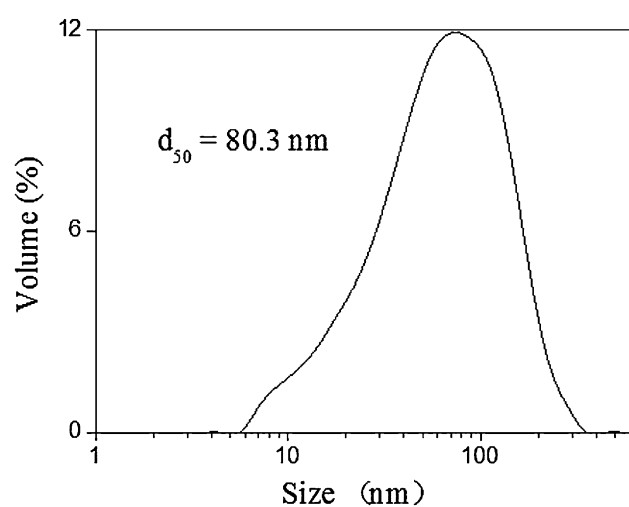
at 100°C and 4.2 MPa . Subsequently, the CO_2 was cooled down by water with a temperature range of $2\text{--}6^\circ\text{C}$ and a pressure of 20.0 MPa was applied. The mixture was pre-heated to 70°C , and put into the drying tower, herein the temperature was kept at 75°C . CO_2 was circulated in the device until the liquid was completely separated from the explosive particles.

2.4 Tests of Mechanical Sensitivities

The friction sensitivity of the samples, I-HMX, O-HMX, F-HMX, was tested at the standard of 90° and 3.92 MPa . Fifty repeating cycles were carried out to obtain the mean explosion probability (\bar{P} , %). The impact sensitivity was characterized by the special height (\bar{H}_{50}), which was statistically calculated through 25 effective test values when the 2.5 kg

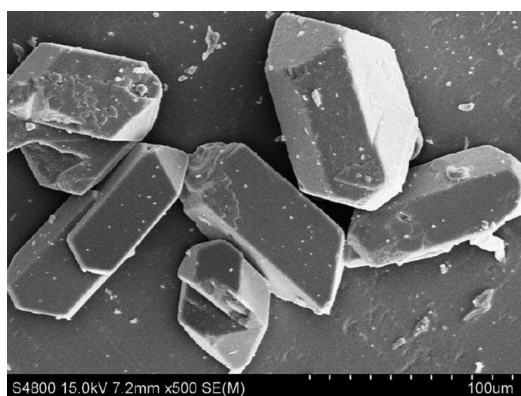


(a) industrial HMX

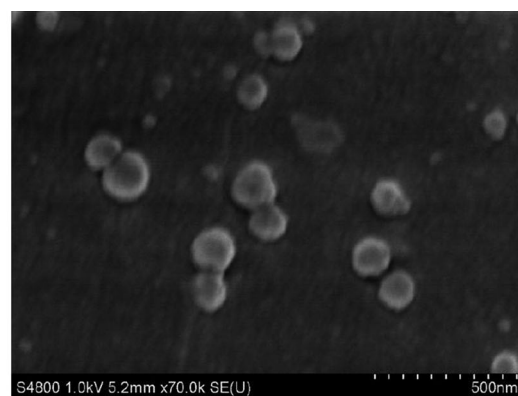


(b) nano HMX

Figure 1. Size distributions of industrial HMX and nano HMX.



(a) industrial HMX



(b) nano HMX

Figure 2. SEM images of industrial HMX and nano HMX.



(a) ethylacetate



(d) water



(b) alcohol



(e) miscible liquid



(c) isopropanol

Figure 3. The dispersion states of HMX dried in different liquids.

drop-hammer was used. The Small Scale Gap Test (SSGT) was taken to measure the shock sensitivity. In this test, the donor column was made of RDX refined by acetone, with a density of 1.48 g cm^{-3} , and the acceptor column had a density of 1.71 g cm^{-3} . The gap thickness (δ) was calculated by 25 effective values.

3 Results and Discussions

3.1 Size Distributions and SEM Images of Industrial HMX and Nano HMX

The size distributions and SEM images of industrial HMX and nano HMX were shown in Figure 1 and Figure 2, respectively.

As shown in Figure 1 and Figure 2, the industrial HMX particles were angularly polyhedral and very heterogeneous having an average particle size of $120.36 \mu\text{m}$ and a wide size distribution. The nano HMX particles were semispherical and had mainly a diameter under 100 nm with narrow size distribution.

3.2 Effect of Liquid on the Dispersion State and Particle Size of Nano HMX

The dispersion states of HMX dried by ordinary drying at 70°C in different liquids are shown in Figure 3.

As shown in Figure 3, the HMX samples were caked seriously after dried in different liquids. When dried in ethyl acetate, some grooves in the sample surface could be observed. When dried in the miscible liquid, there were many big cracks in the surface, and the cracks were successively smaller and less after dried in ethanol, 2-propanol, and water. The different dispersibility of HMX in different liquids resulted in the different states after drying.

The size distributions and the SEM images of HMX obtained by ordinary drying at 70°C in different liquids are shown in Figure 4 and Figure 5.

As shown in Figure 4 and Figure 5, the particles became much bigger presenting wide size distributions after nano HMX was dried in different liquids. The average size was $1.90 \mu\text{m}$ and most of the particles had a diameter of $1\text{--}5 \mu\text{m}$ after drying in ethyl acetate. When dried in alcohol, the average particle size was $1.66 \mu\text{m}$ and mainly under $3 \mu\text{m}$. When dried in 2-propanol, the average particle size was $1.46 \mu\text{m}$. When dried in water, the average particle size was $1.42 \mu\text{m}$ and most particles were under $2 \mu\text{m}$. While it was dried in the miscible liquid, the average particle size was $1.18 \mu\text{m}$ and all of the particles were under $2 \mu\text{m}$.

Nano HMX would be dissolved to some extent in different liquids. When the liquid was removed by evaporation, the nanoparticles tend to agglomerate and grow so that the huge specific surface energy was overcome. The worse the dispersibility, the greater the agglomeration was. The larger the solubility, the stronger the size increment was.

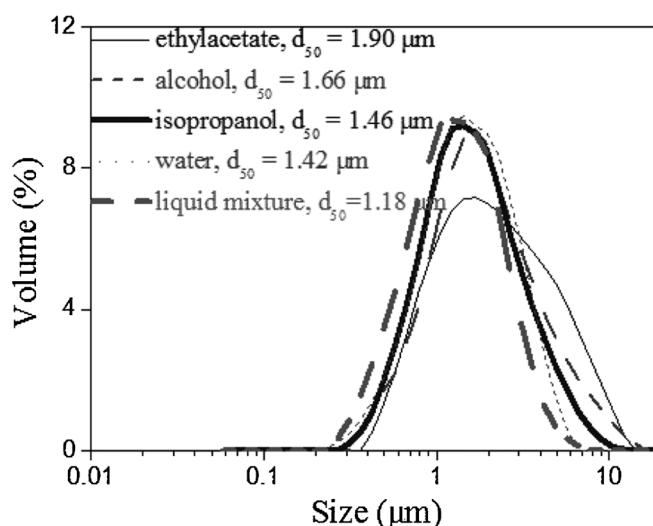


Figure 4. The size distributions of HMX dried in different liquids.

Therefore, various dispersion states and size distributions were exhibited after dried in different liquids.

3.3 Effect of Temperature on the Dispersion State and Particle Size of Nano HMX

The dispersion states of HMX dried by ordinary drying in the miscible liquid at various temperatures are shown in Figure 6. As shown in Figure 6, the HMX samples were caked seriously after dried at various temperatures. The higher temperature, the samples were caked more seriously and the cracks were more and wider.

The size distributions and SEM images of HMX dried by ordinary drying in the miscible liquid at various temperatures are shown in Figure 7 and Figure 8. As shown in Figure 7 and Figure 8, the particles became bigger with wide size distributions after dried at various temperatures. When dried at 90°C , the average particle size was $1.45 \mu\text{m}$ and the particles were mainly under $3 \mu\text{m}$. The average particle size was $1.18 \mu\text{m}$ after dried at 70°C . With the further reducing of the drying temperatures, the average particle size was cut down.

When the drying temperature was increased, the evaporation rate of the liquid was accelerated, the thermal motion of the particles was aggravated, the agglomeration trend was enhanced, and the solubility of nano HMX in the miscible liquid was strengthened. So the average particle size was increased and the caked phenomenon was more serious.

3.4 Effect of Drying Mean on the Dispersion State and Particle Size of Nano HMX

The dispersion states of HMX dried in the miscible liquid under differentiated means are shown in Figure 9. As shown in Figure 9, when nano HMX addressed in vacuo

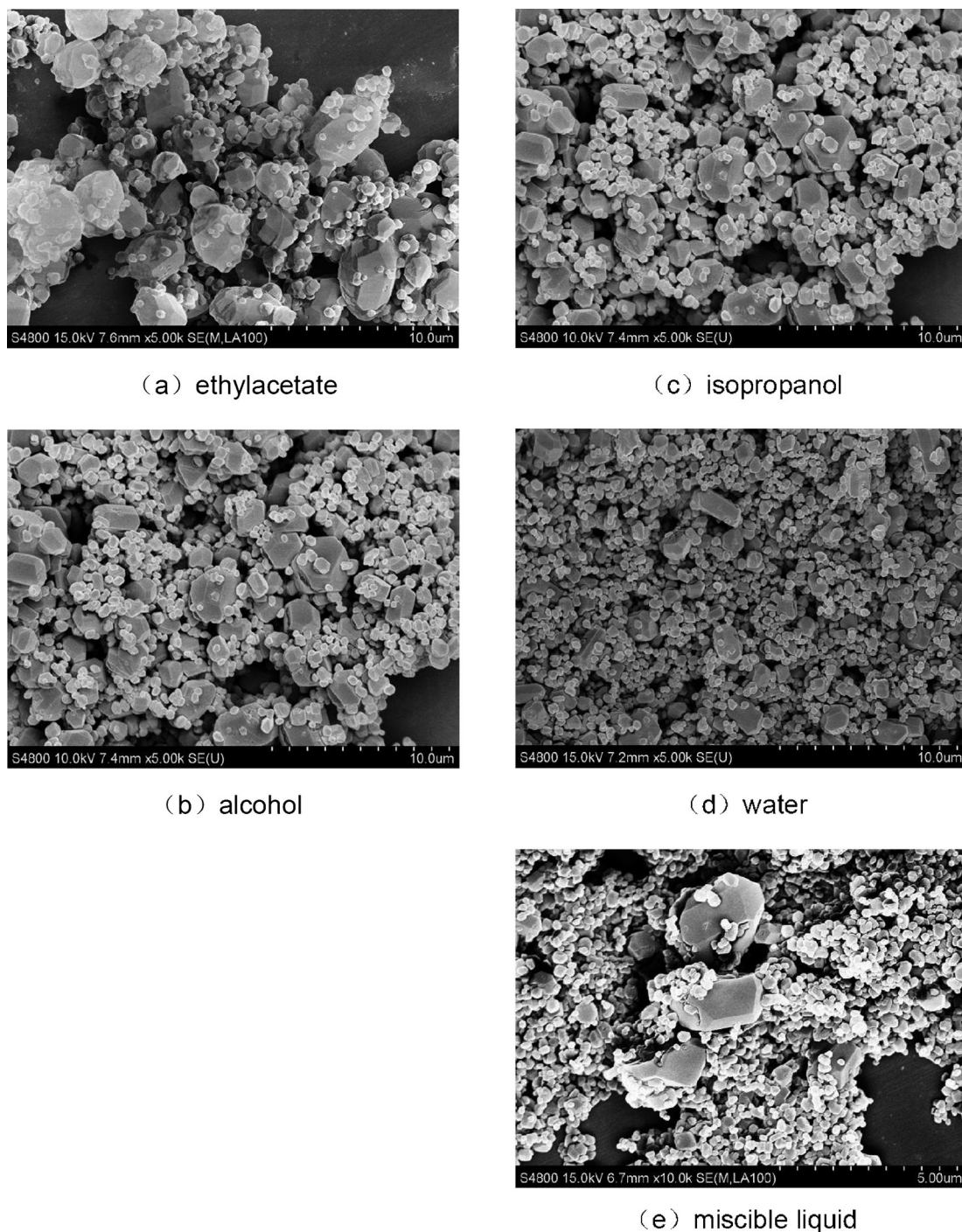


Figure 5. The SEM images of HMX dried in different liquids.

drying, the samples were caked more seriously exhibiting more and wider cracks than those dried in ordinary drying. The sample was fluffy and there were few granular aggregates after disposed in supercritical drying, furthermore, the sample was very fluffy and the particle dispersion was very good after processed in freeze drying.

The size distributions and SEM images of HMX dried in the miscible liquid under different conditions are shown in Figure 10 and Figure 11. As shown in Figure 10 and Figure 11, after dried in ordinary drying, the average particle size was $1.18\ \mu\text{m}$ and all of the particles were under $2\ \mu\text{m}$. The average particle size was $1.49\ \mu\text{m}$ with some particles bigger than $2\ \mu\text{m}$ even up to $10\ \mu\text{m}$ after addressed

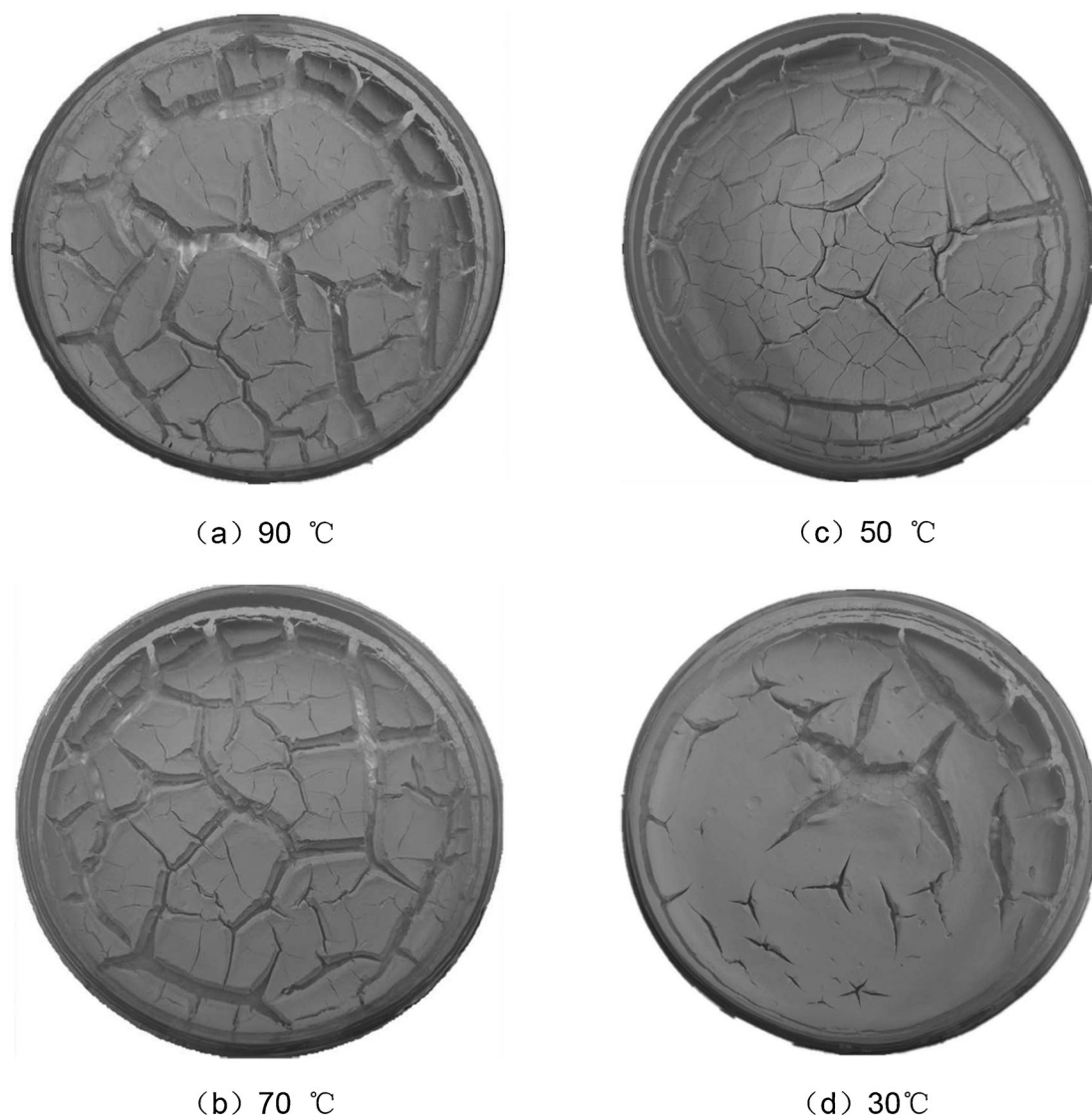


Figure 6. The dispersion states of HMX dried at various temperatures.

in vacuo drying. When disposed in supercritical drying, the size distribution was narrow and most of the particles were in the range of 200–300 nm. While the nano HMX processed in freeze drying, the size distribution was very narrow and the particles were mainly in 100–200 nm.

When addressed in vacuo environment, the boiling point of the liquid was decreased, the evaporation rate was aggravated, the agglomeration trend was enhanced, and the solubility was strengthened. So the sample was caked more seriously with larger particles and wider size distribution than that at room pressure. The effect of supercritical expansion, especially the freezing effect, could prevent the agglomeration and the growth of the nano particles efficiently, so the samples were fluffy, the average particle sizes were small, and the size distributions were narrow.

3.5 Mechanical Sensitivities of HMX Samples

The friction, impact, and shock sensitivities of I-HMX ($d_{50} = 120.36 \mu\text{m}$), O-HMX ($d_{50} = 1.18 \mu\text{m}$) and F-HMX ($d_{50} = 0.16 \mu\text{m}$) were carried out.

As listed in Table 1, when the friction sensitivity was carried out at 90°, 3.92 MPa, the mean explosion probability of

Table 1. The friction sensitivities of HMX samples.

| Samples | 90°, 3.92 MPa $\bar{P}/[\%]$ |
|---------|---------------------------------|
| I-HMX | 86 |
| O-HMX | 72 |
| F-HMX | 58 |

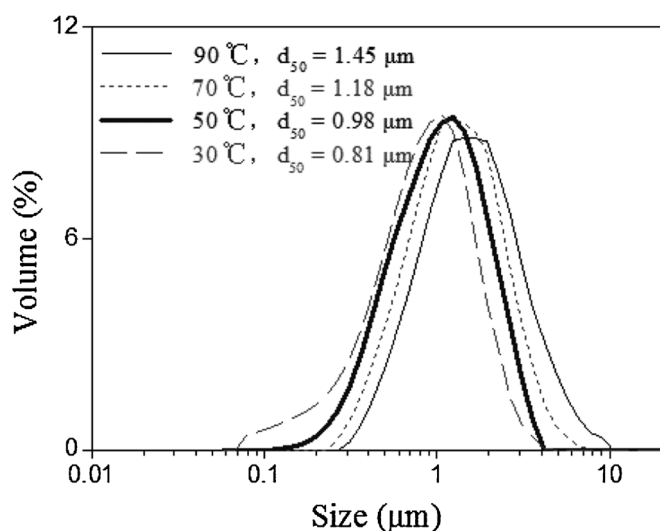


Figure 7. The size distributions of HMX dried at different temperatures.

F-HMX was 14% lower than that of O-HMX, which was still lower by 14% than that of I-HMX.

As listed in Table 2, when the special height was characterized at 2.5 kg, it was increased 4.5 cm for O-HMX and

18.9 cm for F-HMX, compared with I-HMX, in other words, the impact sensitivity was lower by 10.2% and 42.8%, respectively. Additionally, the standard deviation ($S_{dev.}$) was decreased with the reducing of the average particle size (d_{50}), which revealed better detonation stability to impact when the HMX particle size was cut down.

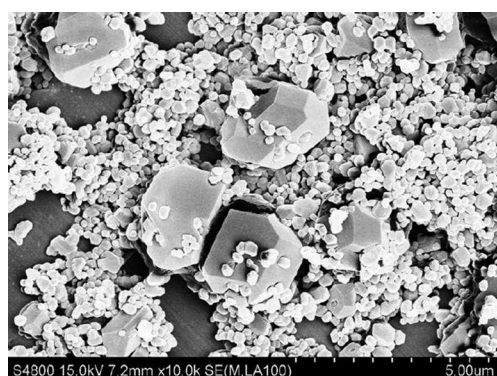
As listed in Table 3, compared with I-HMX, the gap thickness was 5.53 mm lower for O-HMX and 7.88 mm lower for

Table 2. The impact sensitivities of HMX samples.

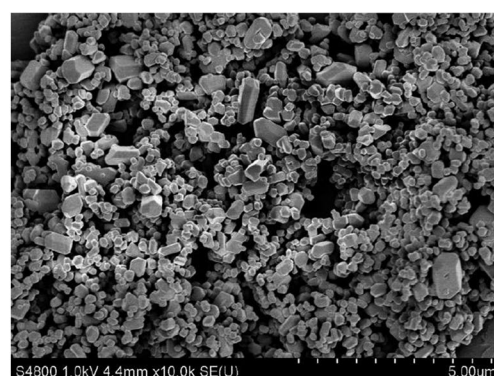
| Samples | 2.5 kg hammer | |
|---------|----------------|------------|
| | H_{50} /[cm] | $S_{dev.}$ |
| I-HMX | 44.1 | 0.15 |
| O-HMX | 48.6 | 0.12 |
| F-HMX | 63.0 | 0.09 |

Table 3. The shock sensitivities of HMX samples.

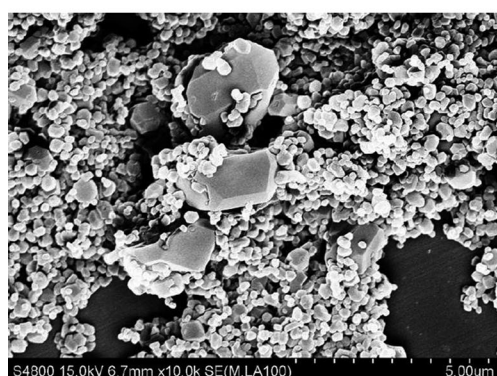
| Samples | Gap thickness δ | |
|---------|------------------------|------------|
| | δ /[mm] | $S_{dev.}$ |
| I-HMX | 13.96 | 0.40 |
| O-HMX | 8.43 | 0.40 |
| F-HMX | 6.08 | 0.32 |



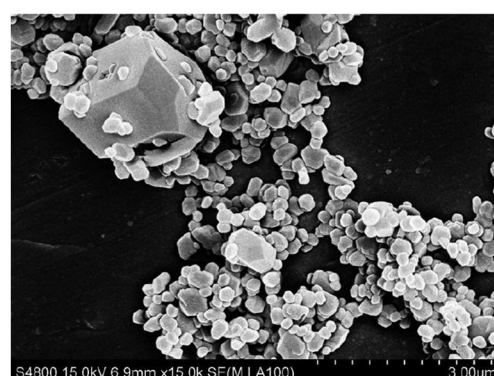
(a) 90 °C



(c) 50 °C



(b) 70 °C



(d) 30 °C

Figure 8. The SEM images of HMX dried at various temperatures.

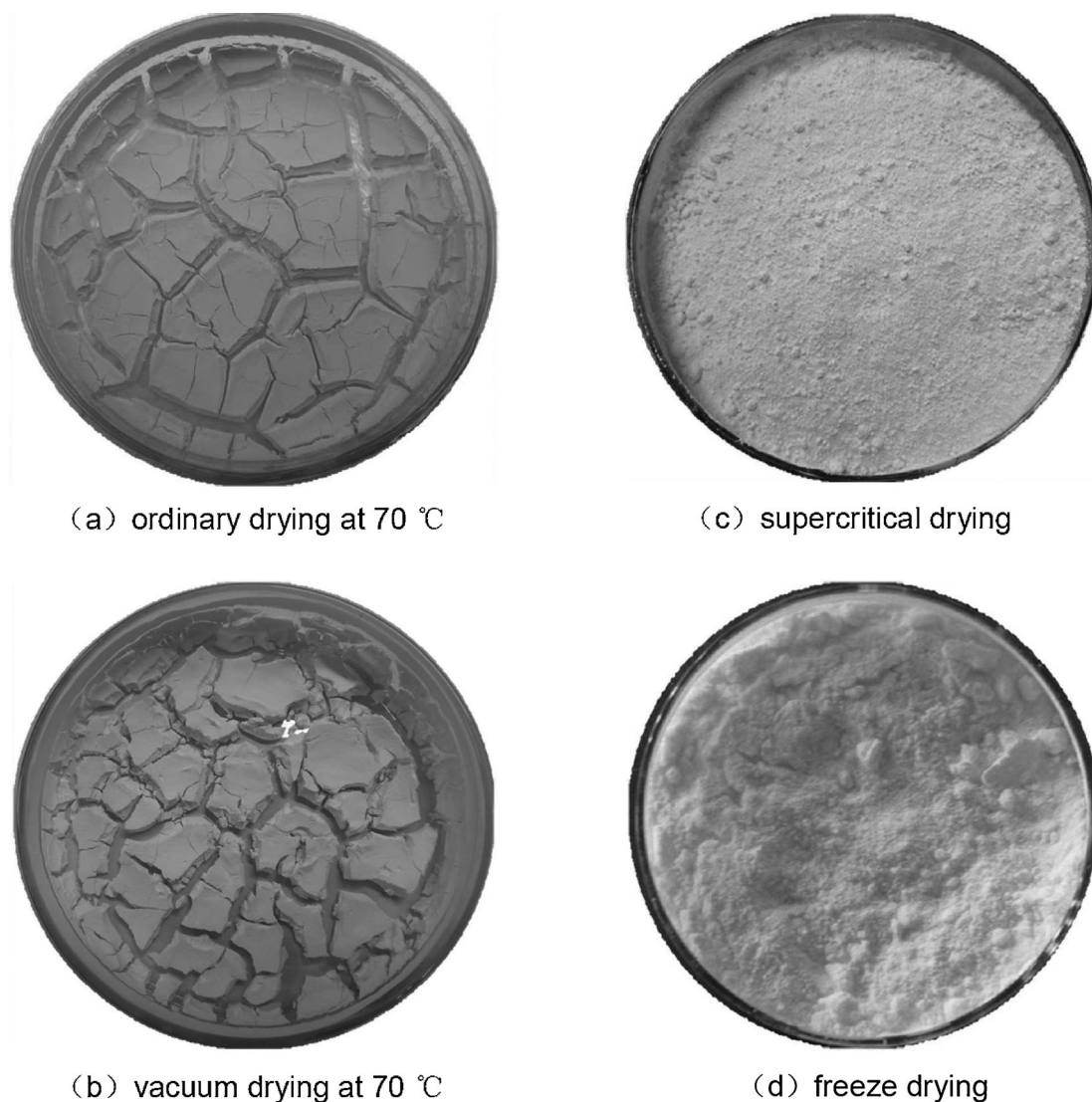


Figure 9. The dispersion states of HMX dried under differentiated means.

F-HMX, which was meaning that the shock sensitivity was lower by 39.6% and 56.4% for each other. Furthermore, the standard deviation (S_{dev}) exhibited a decreased trend with the reducing of the average particle size (d_{50}), which stated that the detonation stability to shock of HMX was better if the particle size was decreased.

4 Conclusions

The samples were caked seriously and the particles were agglomerated to grow bigger after nano HMX was dried by ordinary drying or vacuum drying. The larger the solubility, the worse the dispersibility, or the higher the temperature, the bigger the average particle size and the wider the appearing cracks were. The effect of supercritical expansion, especially the freezing effect, could prevent efficiently ag-

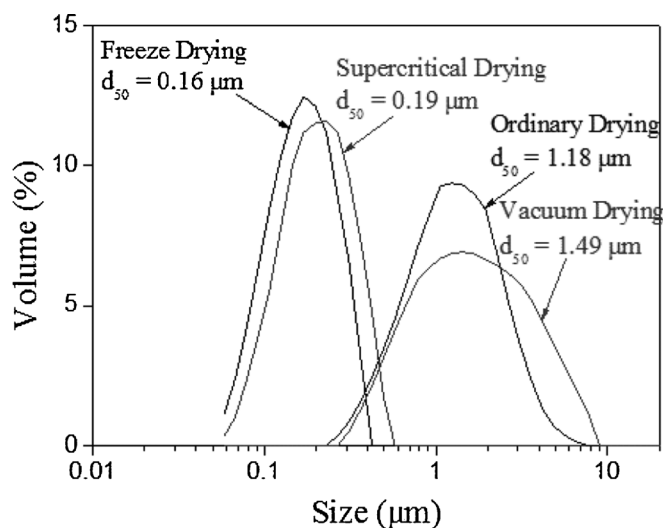
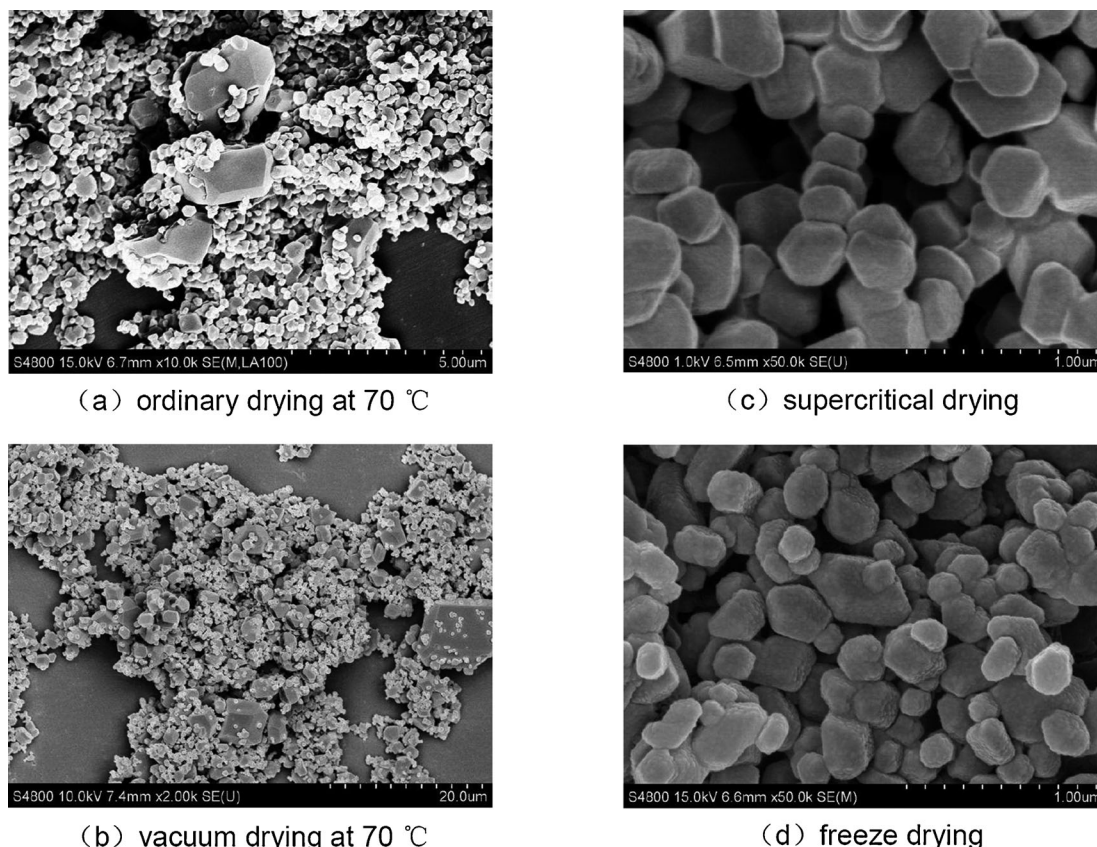


Figure 10. The size distributions of HMX dried under different conditions.



(a) ordinary drying at 70 °C

(c) supercritical drying

(b) vacuum drying at 70 °C

(d) freeze drying

Figure 11. The SEM images of HMX dried under different conditions.

glomeration and growth of the nanoparticles. The mechanical sensitivities were decreased and the detonation to impact or shock was stabilized with reducing the d_{50} .

The samples exhibited various dispersion states, particle sizes, and mechanical sensitivities after drying under different conditions. The small processing capacity of the supercritical drying restricts its application, and the proper way to extract nano HMX is freeze drying. It is promising to promote the large-scale applications of nano HMX, such as insensitive PBX and insensitive CMDB.

Symbols and Abbreviations:

| | |
|-----------------------|---|
| I-HMX: | Industrial HMX sample |
| O-HMX: | Dried samples of nano HMX by ordinary drying at 70 °C |
| F-HMX: | Dried samples of nano HMX by freeze drying |
| Ordinary drying: | Dried in a water bath oven |
| Vacuum drying: | Addressed in a vacuum oven |
| Supercritical drying: | Disposed in a supercritical drying equipment |
| Freeze drying: | Processed in a vacuum freeze drying device |

Miscible liquid:

Mixture of deionized water, ethanol, and 2-propanol, with the volume ratio of 10:10:1.

References

- [1] B. Nouguez, B. Mahe, P. O. Vignaud, Cast PBX Related Technologies for IM Shells and Warheads, *Sci. Technol. Energ. Mater.* **2009**, 70, 135–139.
- [2] R. Menikoff, Comparison of Constitutive Models for Plastic-bonded Explosives, *Combust. Theory Model.* **2008**, 12, 73–91.
- [3] D. J. Funk, F. Calgaro, R. D. Averitt, M. L. T. Asaki, A. J. Taylor, THz Transmission Spectroscopy and Imaging: Application to the Energetic Materials PBX 9501 and PBX 9502, *Appl. Spectrosc.* **2004**, 58, 428–431.
- [4] V. A. Strunin, L. I. Nikolaeva, Combustion Mechanism of HMX and HMX and Possibilities of Controlling the Combustion Characteristics of Systems Based on Them, *Combust. Explos. Shock Waves (Engl. Transl.)* **2013**, 49, 53–63.
- [5] E. Landsem, T. L. Jensen, F. K. Hansen, E. Unneberg, T. E. Kristensen, Neutral Polymeric Bonding Agents (NPBA) and Their Use in Smokeless Composite Rocket Propellants Based on HMX-GAP-BuNENA, *Propellants Explos. Pyrotech.* **2012**, 37, 581–591.
- [6] R. Dubey, P. Srivastava, I. P. S. Kapoor, G. Singh, Synthesis Characterization and Catalytic Behavior of Cu Nanoparticles on the

- Thermal Decomposition of AP, HMX, NTO and Composite Solid Propellants, Part 83, *Thermochim. Acta* **2012**, 549, 102–109.
- [7] Q. L. Yan, X. J. Li, Y. Wang, W. H. Zhang, F. Q. Zhao, Combustion Mechanism of Double-base Propellant Containing Nitrogen Heterocyclic Nitroamines (I): The Effect of Heat and Mass Transfer to the Burning Characteristics, *Combust. Flame* **2009**, 156, 633–641.
- [8] S. C. Lu, Y. B. Jia, Q. Y. Yang, B. C. Wang, Effect of Catalyst ($\text{SnO}_2/\text{PbO}_2/\text{Pb/Sn}$) on Combustion Performance of Al/HMX/CMDB Propellant, *7th International Autumn Seminar on Propellants, Explosives and Pyrotechnics*, Beijing, China, October 25–28, **2005**, p. 708–712.
- [9] M. E. Afshani, A. Sahafian, A. Hamidi, Experimental Research on Composite Modified Double Base Propellants, Theory and Practice of Energetic Materials, *5th International Autumn Seminar on Propellants, Explosives and Pyrotechnics (IASPEP)*, Guilin, China, October 15–18, **2003**, p. 491–498.
- [10] X. L. Song, Y. Wang, C. W. An, X. D. Guo, F. S. Li, Dependence of Particle Morphology and Size on the Mechanical Sensitivity and Thermal Stability of Octahydro-1,3,5,7-tetranitro-1,3,5,7-tetrazocine, *J. Hazard. Mater.* **2008**, 159, 222–229.
- [11] X. L. Song, F. S. Li, Dependence of Particle Size and Size Distribution on Mechanical Sensitivity and Thermal Stability of Hexahydro-1,3,5-trinitro-1,3,5-triazine, *Defence Sci. J.* **2009**, 59, 37–42.
- [12] C. R. Siviour, M. J. Gifford, S. M. Walley, W. G. Proud, J. E. Field, Particle Size Effects on the Mechanical Properties of a Polymer Bonded Explosive, *J. Mater. Sci.* **2004**, 39, 1255–1258.
- [13] X. L. Song, F. S. Li, J. L. Zhang, X. D. Guo, C. W. An, Y. Wang, Influence of Particle Size, Morphology and Size Distribution on the Safety and Thermal Decomposition Properties of RDX, *J. Solid Rocket Technol.* **2008**, 31, 168–172.
- [14] X. N. Zhang, G. G. Xu, J. P. Xu, W. M. Wang, A Study about Impact Sensitivity of Ultrafine HMX and HMX, *Chin. J. Explos. Propellants* **1999**, 22, 33–36.
- [15] J. Liu, J. B. Zeng, Qing Li, L. X. Wang, S. Zhou, W. Jiang, F. S. Li, Mechanical Pulverization for Nano HMX and Study on Its Mechanical Sensitivities, *Chin. J. Explos. Propellants* **2012**, 35, 12–14.
- [16] Y. X. Zhang, D. B. Liu, C. X. Lv, Preparation and Characterization of Reticular Nano-HMX, *Propellants Explos. Pyrotech.* **2005**, 30, 438–441.
- [17] Y. Bayat, S. M. Pourmortazavi, H. Iravani, H. Ahadi, Statistical Optimization of Supercritical Carbon Dioxide Antisolvent Process for Preparation of HMX Nanoparticles, *J. Supercritical Fluids* **2012**, 72, 248–254.
- [18] J. Liu, W. Jiang, F. S. Li, Y. Wang, S. Zhou, K. W. Bao, Preparation and Study on Nano Octahydro-1,3,5,7-tetranitro-1,3,5,7-tetrazocine, *Acta Armamentarii* **2013**, 34, 174–180.
- [19] F. S. Li, Y. Yang, H. Y. Liu, W. Jiang, Bi-directional Rotation Mill, Chinese Patent: CN2766956, Nanjing University of Science and Technology, Nanjing, China, **2006**.

Received: May 1, 2013
Revised: June 3, 2013
Published online: July 3, 2013